

Electromagnetic Excitation of Unstable Nuclei*

C. A. Bertulani[†]

*Instituto de Física, Universidade Federal do Rio de Janeiro
Cx. Postal 68528, 21945-970, Rio de Janeiro, RJ, Brazil*

Received May 21, 1996.

We discuss the perspectives of using the Coulomb excitation mechanism to study the properties of unstable nuclei.

I. Introduction

Unstable nuclei are often studied in reactions induced by secondary beams. Examples of such reactions include elastic scattering, fragmentation and Coulomb excitation in collisions with very heavy targets^[1]. Coulomb excitation is especially useful, since the interaction mechanism is well known. The cross sections for Coulomb excitation of radioactive beams yield valuable information on the intrinsic electromagnetic moments of these nuclei. Such information is hard to obtain with other methods due to the short lifetime of unstable projectiles. When first-order perturbation theory is valid, it is easy to show that Coulomb excitation and the excitation induced by real photons are proportional to each other^[2], i.e.,

$$\sigma_c = \sum_{\pi\lambda} \int N_{\pi\lambda}(E_x) \sigma_{\gamma}^{\pi\lambda}(E_x) \frac{dE_x}{E_x}, \quad (1)$$

where E_x is the excitation energy and $\sigma_{\gamma}^{\pi\lambda}(E_x)$ is the photonuclear cross section for the multipolarity $\pi\lambda$ ($\pi = E$ or M , and $\lambda = 1, 2, \dots$). This relation is exact, valid for all bombarding energies. Due to the short wavelength of the bombarding nuclei, semiclassical methods are appropriate to calculate the equivalent photon numbers $N_{\pi\lambda}(E_x)$. In ref. [3] a general method was developed to calculate $N_{\pi\lambda}(E_x)$ for all energies, including kinematical and relativistic effects. At relativistic energies $N_{\pi\lambda}(E_x)$ can be calculated by simple analytical formulas^[4].

Experiments with radioactive beams are often restricted to the measurement of total cross sections. A limited but useful information on the excitation mechanisms can be learned in this way. A classical example is the Coulomb breakup of ^{11}Li . This nucleus is very loosely bound (the separation energy of the last two neutrons is $S = 0.35$ MeV) and does not have other bound states. The Coulomb breakup of this nucleus proceeds directly to the continuum and is dominated by electric dipole transitions. It was soon realized that, in order to explain the large Coulomb breakup cross sections, the matrix element $\langle \text{cont.} | \mathcal{O}(E1) | g.s. \rangle$ should be large in magnitude for energies close to the threshold^[5]. This fact led some authors to assume the existence of a resonant state in ^{11}Li . However, the breakup to a structureless continuum also yields large Coulomb breakup cross sections. This happens because the binding energy of this nucleus is very small and Coulomb excitation favors low energy excitations. In Fig. 1 we show the dipole response function $dB(E1)/dE_x \propto | \langle \text{cont.} | \mathcal{O}(E1) | g.s. \rangle |^2$ calculated with the cluster model^[6]. For a comparison we also show the well-known electric dipole response function in lead, which is dominated by the giant resonance at $E_x = 13.5$ MeV. One sees that the excitation strength in ^{11}Li is large close to the particle emission threshold - its integrated value being approximately a factor 20 smaller than the integrated dipole response in Pb.

*Supported in part by the Brazilian funding agencies CNPq and FINEP.

[†]E-mail: bertu@if.ufrj.br

While the response function in Pb is well described by a Lorentzian shape, the form of the response function in ^{11}Li is not well known, except perhaps for its position and total strength. The cluster model yields the simple form^[6]:

$$\frac{1}{e^2} \frac{dB(E1)}{dE_x} = C \frac{\sqrt{S}(E_x - S)^{3/2}}{E_x^4} \quad (2)$$

where C is an adjustable constant. From the magnitude of the Coulomb breakup cross sections for ^{11}Li projectiles, a value $C = 4.01 \text{ fm}^2/\text{MeV}$ is obtained. The peak of this function occurs at $E_x = (8/5)S$, i.e., at an excitation energy of $E_x = 0.56 \text{ MeV}$. The form of the response function (2) results from two assumptions: (a) an extended wavefunction of the halo neutrons in ^{11}Li , and (b) a structureless continuum. It is peaked at low energies because of the small separation energy of the halo neutrons.

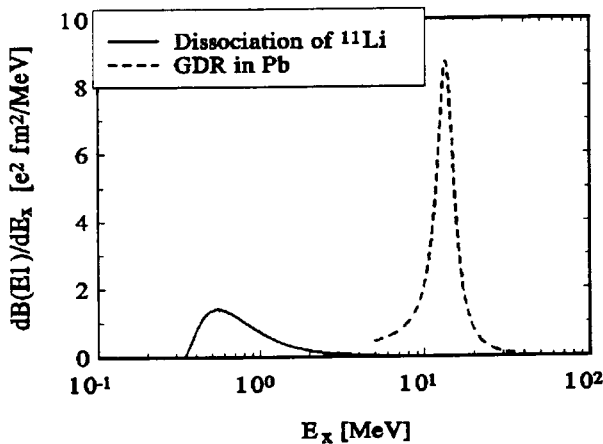


Figure 1. Dipole response function of ^{11}Li (solid line) and of ^{208}Pb (dashed line).

The magnitude of the Coulomb excitation cross sections depends on the dipole photonuclear excitation cross section, which is related to the response function by

$$\sigma_\gamma^{E1}(E_x) = \frac{16\pi^3}{9} \left(\frac{E_x}{\hbar c} \right) \frac{dB(E1)}{dE_x}. \quad (3)$$

The factor E_x on the r.h.s. favors the excitation of high-lying states. However, the electric dipole virtual photon numbers, $N_{E1}(E_x)$, peak at low energies. At low bombarding energies this effect is larger^[2]. In Fig. 2 we plot the breakup cross sections for the excitation of ^{11}Li projectiles incident on lead, as a function

of the bombarding energy per nucleon. For a comparison, we show the cross section for the excitation of the giant dipole resonance in lead projectiles. The cross section for the excitation (breakup) of ^{11}Li is largest at $E_{\text{Lab}} \simeq 10 \text{ MeV/A}$. At very small energies the Coulomb field changes adiabatically resulting in small cross sections. The cross sections increase with bombarding energy because the function $N_{E1}(E_x)$ become more flat. With further increase of the bombarding energy the excitation cross section of ^{11}Li decreases, while the excitation of the giant dipole resonance in lead increases, due to the increasing number of virtual photons of large energies^[4].

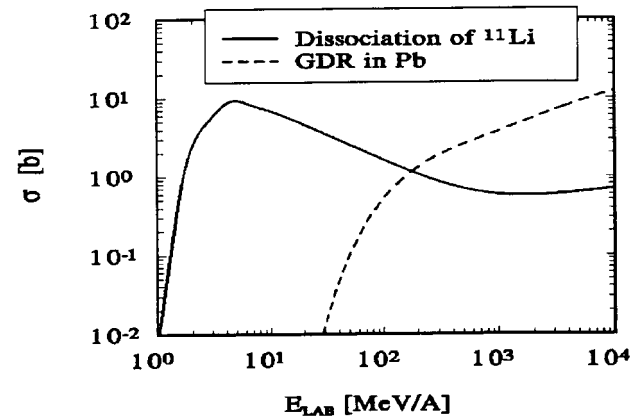


Figure 2. Coulomb excitation cross sections of ^{11}Li projectiles (solid line), and of the giant dipole resonance in Pb projectiles (dashed line) incident on lead targets, respectively.

The measurement of excitation cross sections provides a limited tool for studies of the structure of unstable nuclei. In the case of stable nuclei the analysis of angular distributions in inelastic scattering has been a major technique to access additional information on nuclear structure. It was in this way that the giant monopole resonance could be identified in angular patterns which included competing processes, like the excitation of the giant quadrupole resonance. Inelastic scattering of unstable nuclei has been exploited in ref. [7]. For loosely bound systems inelastic scattering patterns are rather simple because Coulomb excitation dominates the scattering. This is shown in Fig. 3 where the differential cross section for the breakup of ^{11}Li and for the excitation of lead projectiles incident on lead targets at 640 MeV/nucleon (SIS energies at the GSI/Darmstadt) is shown as a function of the

scattering angle. The basic feature is that the angular distribution of ^{11}Li breakup is strongly peaked at the forward direction. Due to its looseness, most of the projectiles disrupt at large impact parameters for which the scattering angle is small. To excite the giant dipole resonance in lead a larger excitation energy is needed. This is only achieved in collisions at small impact parameters for which the scattering angle is larger. The position of the peak in the angular distribution is an increasing function of the excitation energy and a decreasing function of the bombarding energy. Also shown in Fig. 3 are the calculations performed with semiclassical methods (dashed lines)^[8]. These calculations are quite simple to perform and provide a good description of the scattering below the grazing angle where the nuclear absorption processes set in.

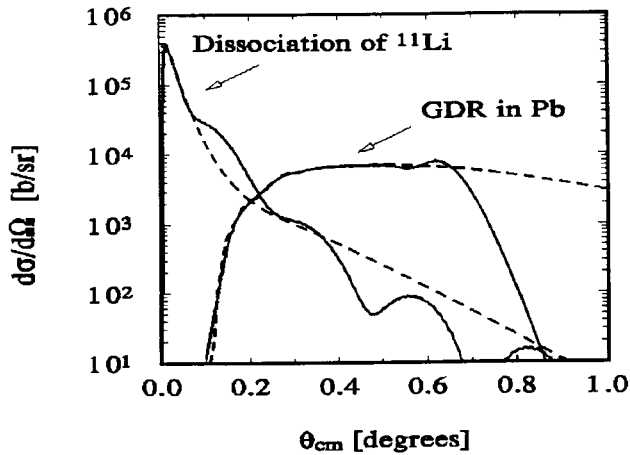


Figure 3. Angular distribution for the breakup of ^{11}Li projectiles and for the excitation of the GDR in lead projectiles incident on lead targets at 640 MeV.A. The solid (dashed) lines are quantum (semiclassical) calculations.

An important use of Coulomb excitation in reactions with radioactive beams occurs when a group of excited states are coupled. In ref. [9] the transition from the ground state (a parity-inverted $\frac{1}{2}^+$ state) of ^{11}Be to the continuum (with threshold at 504 keV) was studied with the Coulomb excitation technique and a good agreement with the form of the response function given by eq. (2) was found. The value $C = 3.73 \pm 0.7 \text{ fm}^2/\text{MeV}$ gives a good fit to the experimental data. The factor C depends essentially on two parameters: (a) the spectroscopic factor of the $n+^{10}\text{Be}$ system, and (b) the effective range of the nuclear interaction. In the experiment of ref. [9], a value close to unity for the

spectroscopic factor and an effective range of 4 fm was found to fit the experimental results.

In ref. [10] the Coulomb excitation of the $1/2^-$ state at 320 keV (the only excited state in ^{11}Be) was studied in collisions of 45 MeV. A ^{11}Be beams on ^{208}Pb targets. Amazingly, it was found that the measured cross section, $191 \pm 26 \text{ mb}$, is a factor 2 smaller than that expected from first order perturbation theory, using $B(E1) = 0.116 \pm 0.012e^2 \text{ fm}^2$. This $B(E1)$ -value is an average over three distinct experiments which yield the lifetime of 166 ± 15 .

The reason for the above mentioned discrepancy could be the coupling of the bound states in ^{11}Be and the continuum, or the contribution from nuclear excitation causing a destructive Coulomb-nuclear interference^[10]. We investigate these possibilities using a semiclassical coupled-channels approach to the Coulomb and nuclear excitation of the $\frac{1}{2}^-$ state in ^{11}Be . The spin and parities of the states involved imply that the Coulomb dipole excitation corresponds to the largest contribution to the cross section. This has been experimentally observed^[9,10] and is theoretically understood^[11]. A coupled-channels approach to this problem was developed in ref. [12], where a relativistic time dependent Coulomb potential, $V(t)$, was used. The Wigner-Eckart theorem allows us to write the matrix elements $\langle k|V(t)|i \rangle$ in terms of the $B(E; M\lambda)$ -values for the electromagnetic multipole transitions. For the transition $\frac{1}{2}^+ \rightarrow \frac{1}{2}^-$ we use the previously mentioned $B(E1)$ -value. The continuum can be treated by means of a discretization procedure so that the $B(E1)$ -values from the bound states to the n th state in the continuum are given by

$$B(E1; i \rightarrow n) = \Delta E_x \cdot \left. \frac{dB(E1, E_x)}{dE_x} \right|_{E_x = E_n}, \quad (4)$$

which can be calculated with help of eq. (2). Above, ΔE_x is the spacing in the continuum energy mesh. In our numerics we use $\Delta E_x = 0.3 \text{ MeV}$, and a total of 10 discretized continuum states. This mesh covers the most important part of the continuum dipole response function in ^{11}Be [9]. A phase convention for the nuclear states can be found so that the reduced matrix elements $\langle I_f M_f || \mathcal{M}(E; M\lambda) || I_i M_i \rangle$ are real^[13]. In the present problem the sign of the matrix elements do

not appreciably affect the results. Then one can set all matrix elements as positive.

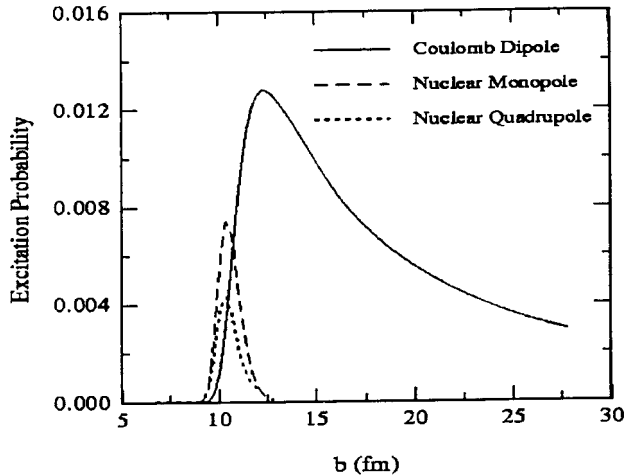


Figure 4. Excitation probability of the dipole, monopole, and quadrupole transitions in ^{11}Be by the Coulomb and the nuclear interaction and as a function of the impact parameter.

The integrated dipole response in the continuum is obtained from eq. (2) as

$$B(E1; i \longrightarrow \text{cont.})/e^2 = \frac{\pi C}{16S}, \quad (5)$$

where i stands for one of the two bound states in ^{11}Be . Using the experimental value of C , we get $B(E1; \frac{1}{2}^+ \longrightarrow \text{cont.}) = 1.45e^2 \text{ fm}^2$, for the ground state, and $B(E1; \frac{1}{2}^- \longrightarrow \text{cont.}) = 4.06e^2 \text{ fm}^2$ for the first excited state.

With respect to the nuclear interaction in peripheral collisions, one expects that the most relevant contributions arise from the monopole and quadrupole isoscalar excitation modes. Isovector excitations are strongly suppressed^[14] due to the approximate charge independence of the nuclear interaction. We adopt the folding optical potential of ref. [7]. For the ground state density of ^{11}Be we use the results^[7] of the Hartree-Fock formalism with Skyrme interaction, and for ^{208}Pb we take a Fermi density with radius $R = 6.67 \text{ fm}$ and diffuseness $a = 0.55 \text{ fm}$. The monopole and quadrupole transition potentials were calculated with the Tassie model, as explained in ref. [7]. In terms of the optical potential $U_{opt}(r)$, they can be written

$$V_N(r) = \begin{cases} \alpha_0[3U_{opt}(r) + r dU_{opt}(r)/dr], & \text{for monopole;} \\ (\delta_2/\sqrt{5})[dU_{opt}(r)/dr], & \text{for quadrupole,} \end{cases} \quad (6)$$

where α_0 and δ_2 are parameters to fit inelastic scattering data. Since there are no such data on ^{11}Be , we arbitrarily choose $\alpha_0 = 0.1$ and $\delta_2 = 1 \text{ fm}$. These values correspond to about 5% of the energy-weighted sum rule, if a state at 1 MeV excitation energy is assumed, and should be reasonable for a qualitative calculation. The nuclear couplings are given a time-dependence through the application of a Lorentz boost on the system. This amounts to multiplying eq. (6) by the Lorentz factor γ , and using $r = \sqrt{b^2 + \gamma^2 v^2 t^2}$. The cross section to excite the state k is calculated from the relation

$$\sigma_k = 2\pi \int db b |a_k(b)|^2 \exp[(2/\hbar v) \text{Im}\{ \int dz U_{opt}(r) \}], \quad (7)$$

where $\mathbf{r} = (\mathbf{b}, z)$, and $a_k(b)$ is the occupation amplitude of the state k calculated by the coupled-channels method. The exponential term accounts for the strong absorption along the classical trajectory.

Table I shows the result of the calculation where “Theory (1)” is the first order perturbation theory. In the column “Theory (2)”, reorientation effects caused by the magnetic dipole transitions $\frac{1}{2}^+ \longrightarrow \frac{1}{2}^+$ are included. For this purpose, the Schmidt value $B(M1, \frac{1}{2}^+ \longrightarrow \frac{1}{2}^+) = 0.087 e^2 \text{ fm}^2$ is used, and the magnetic dipole coupling is calculated through the same procedure as that employed for V_{E1} [15]. We note that this effect can be neglected, since it causes a negligible change in the cross sections. On the other hand, the inclusion of the coupling to the continuum yields more sizeable effects. The cross section for the excitation of the $\frac{1}{2}^-$ state decreases by about 4%. This reduction is, however, still too small to explain the discrepancy between experiment and theory. Finally, in the column “Theory (4)”, we present effects of nuclear excitation. These effects are also very small. The reason is that the nuclear interaction is limited to a very small impact parameter region, around the grazing value, as illustrated in Fig. 4. The cross sections for the nuclear excitation of monopole and quadrupole states are respectively 7.07 mb and 6.22 mb. A second reason for this fact is that Coulomb-nuclear interference only appears for high-order transitions, i.e., those involving many excitation steps. This occurs because the Coulomb coupling is dominated by the dipole term

Table I

	Exp.	Theory (1)	Theory (2)	Theory (3)	Theory (4)
$\sigma_{1/2^-}$ (mb)	191 ± 26	405.81	405.80	388.2	390.2
$\sigma_{cont.}$ (mb)	–	–	–	334.5	335.2

while the nuclear coupling is dominated by monopole and quadrupole excitation. In table I we also show the dissociation cross section, $\sigma_{cont.}$. It is of the same magnitude as $\sigma_{1/2^-}$. Perhaps, a further increase of the transition probability from the excited state to the continuum would occur in the presence of a resonance in ^{14}Be close to the threshold. However, presently, this hypothesis lacks experimental evidence^[9]. Further studies are needed to clarify this matter.

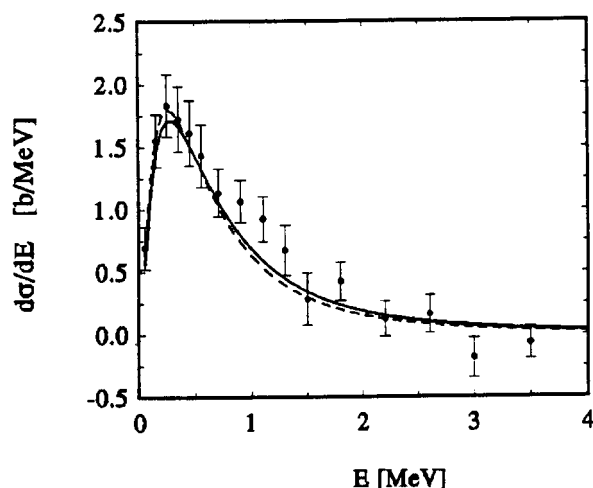


Figure 5. Differential cross section for the breakup of 72 MeV/nucleon ^{11}Be projectiles incident on lead targets, as a function of the relative energy of the fragments.

The Coulomb reacceleration effect observed in ref. [16] presents another tool to study unstable nuclei. This effect consists in the reacceleration of the charged fragments by the Coulomb field of the target after the breakup. A possible use of this effect is to study if the breakup proceeds through the excitation of a resonant state, or through a direct breakup to a structureless continuum. In the first case the excited nucleus decays far from the region where the Coulomb field is strong due to the resonance lifetime and no reacceleration effect should be observed^[17]. The positive evidence of the reacceleration effect presented in ref. [16] implies that the breakup proceeds to a structure-

less continuum. Theoretical calculations give support to the existence of this effect^[11,18]. However, the effect depends strongly on the system. While it is important for ^{11}Li Coulomb breakup, as in the experiment of ref. [16], it is only marginal for the Coulomb breakup of ^{11}Be , as observed in ref. [9]. This can be seen in Fig. 5 where we plot the relative energy distribution of the fragments ($n+^{10}\text{Be}$) for a collision of (72 MeV/nucleon) ^{14}Be projectiles with lead targets. The solid line corresponds to first order perturbation theory, and the dashed line to a calculation which solves time-dependent Schrödinger equation non-perturbatively^[11]. The data are from ref. [9]. This is the reason why we neglected the continuum-continuum transitions in the coupled-channels analysis of the excitation of the $\frac{1}{2}^-$ state in ^{11}Be , since these transitions correspond to the reacceleration effect. Reacceleration effects will be more important at lower bombarding energies, as shown in ref. [11].

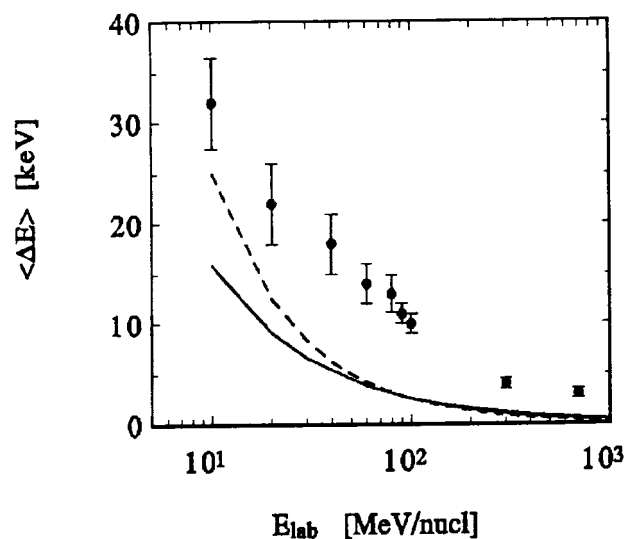


Figure 6. Reacceleration energy in the relative motion of p and ^7Be fragments as a function of the bombarding energy per nucleon of the ^8B projectiles incident on lead targets.

The Coulomb reacceleration effect is also important in another scenario. The validity of first order pertur-

bation theory, leading to the derivation of eq. (1), is important for the feasibility of the Coulomb dissociation method for astrophysical purposes^[19]. One of the reactions of primordial interest, closely related to the solar neutrino problem^[8] is the Coulomb breakup of ^8B projectiles, which leads to information on the rate of proton capture by ^7Be in the Sun. The first breakup experiment with this nucleus is described in ref. [20], and a smaller value of the S-factor for proton capture on ^7Be than those obtained in direct capture experiments was deduced. Further experiments using the Coulomb dissociation method for this reaction are planned. One of the important features to be studied will be the separation of the E2 from the E1 component entering the S-factor^[21]. For the success of these experiments it is important that the final energies of the fragments are not influenced by reacceleration. This seems to be the case for the breakup of ^8B projectiles. In Fig. 6 we show the magnitude of the reacceleration effect as a function of the bombarding energies of ^8B projectiles incident on lead targets^[8]. Different methods have been used in this calculation: (a) a Monte-Carlo calculation assum-

ing classical trajectories for the fragments (described by points with error bars in Fig. 6 - errors bars correspond to numerical uncertainties), (b) an average of Coulomb breakup probabilities folded with classically calculated reacceleration energies^[17], and (c) the solution of the time-dependent Schrödinger equation for the two-body breakup problem^[11]. One sees that in all cases the reacceleration effect is small compared to the relative energy of the fragments which one wants to measure, $E_{rel} \simeq 100$ keV. We note from Fig. 6 that the reacceleration effect decreases with the bombarding energy thus favoring experiments at some hundreds of MeV per nucleon which can be achieved at the SIS, GSI/Darmstadt.

The experiments with momentum distributions of the fragments in reactions with secondary nuclear beams are very popular because they are rather simple. One hopes to get information about the halo size of unstable nuclei from the width of the distributions. The singles spectra of fragment b when fragment x is stripped from the projectile $a = b + c$ in high energy collisions is given by [22]

$$\frac{d\sigma}{d\Omega_b dE_b} = \rho(E_b) \frac{2E_x}{\hbar v_{ak_x}} \int d^2b_x |\phi_a(\mathbf{q}, \mathbf{b}_x)|^2 [1 - |S_{xA}|^2], \quad (8)$$

where

$$\phi_a(\mathbf{q}, \mathbf{b}_x) = \int d^3r_b \exp(i\mathbf{q}_b \cdot \mathbf{r}_b) S_{bA}(b_b) \phi_a(\mathbf{r}_b - \mathbf{r}_x). \quad (9)$$

The quantity $S_{iA}(b_i)$ is the S-matrix for the scattering of cluster i ($i = b, x$)-from target A. ϕ_a represents the cluster wave function for the incoming projectile. If one assumes that the fragment b does not interact with the target, i.e., $S_{bA}(b_b) = 1$, one finds

$$\frac{d\sigma}{d\Omega_b dE_b} = \sigma(E_b) \sigma_{xA}^R |\phi_a(\mathbf{q}_b)|^2, \quad (10)$$

where σ_{xA}^R is the total reaction cross section of fragment x with the target A, and $\phi_a(\mathbf{q}_b)$ is the Fourier transform of $\phi_a(\mathbf{r}_b - \mathbf{r}_x)$ with respect to \mathbf{q}_b . This result tells us that in the “soft interaction” approximation the stripping mechanism measures the momentum-space internal wave function of the projectile, so that singles spec-

tra of fragment b provides valuable information on the internal structure of the projectile. This is specially useful for the study of extremely short-lived nuclei in secondary beam interactions.

The “soft interaction” model is only a rough approximation to most cases and the elastic scattering of the fragment b on the target has to be included, leading to an unavoidable broadening of the momentum distributions. The physical origin for this broadening is simple diffraction, as an examination of eq. (8) makes clear. For instance, if $S_{bA} = \Theta(b - R)$, the Fourier transform given by this equation would be exactly the Fraunhofer diffraction pattern (as a function of \mathbf{q}_b) of

the “source distribution” $\phi_a(\mathbf{r}_b - \mathbf{r}_x)$. Including the factor $S_{bA}(b_b)$, with $|S_{bA}(b_b)|^2 \leq 1$, effectively decreases the transverse width of the source by eliminating the part that overlaps with the target A , and this will of course broaden the transverse diffraction pattern. We thus conclude that transverse momentum distributions do not directly give information on the projectile wave function, as expected from the simple approach leading to eq. (10).

This broadening makes it harder to extract the internal momentum structure of the projectile. However, since for high-energy collisions the S -matrix S_{bA} does not depend on the longitudinal coordinate, the longitudinal momentum distribution can be shown to be much less modified by the $S_{bA}(b_b)$ -absorption factor^[22]. This is also the case if one includes the Coulomb breakup mechanism. The singles spectra from Coulomb (electric dipole) breakup will be given by

$$\frac{d\sigma_C}{d\Omega_b dE_b} = \sum_{f,m} \text{Const.}(m) \times \left| \int d^3r r Y_{1m}(\mathbf{r}) [\phi_a^f(\mathbf{r})]^* \phi_a^i(\mathbf{r}) \right|^2. \quad (11)$$

Since the operator $rY_{1m}(\mathbf{r})$ is a slowly varying function of \mathbf{r} , the above relation can be shown^[22] to give similar results as eq. (10) if the final wave function of the projectile, $\phi_a^f(\mathbf{r})$, is not strongly modified by final state interactions. In reactions influenced by the Coulomb reacceleration effects, this simple relation fails to exist. We thus conclude that the widths of longitudinal momentum distributions can be associated with the size of halo nuclei, under special conditions. The discussion presented here is somewhat simplified. If one includes other breakup mechanisms, e.g., elastic breakup^[23] or final state interactions, the breakup mechanism is more difficult to understand. However, more detailed calculations^[24,23] have confirmed that transverse momentum distributions are much more difficult to relate to the ground state wave function of the projectile than longitudinal momentum distributions.

References

1. P.G. Hansen, Nucl. Phys. **A553** 89c (1993); C.A. Bertulani, L.F. Canto and M.S. Hussein, Phys. Reports **226**, 281 (1993).
2. C.A. Bertulani and G. Baur, Nucl. Phys. **A442**, 739 (1985).
3. A.N.F. Aleixo and C.A. Bertulani, Nucl. Phys. **A505**, 448 (1989).
4. C.A. Bertulani and G. Baur, Phys. Reports **163**, 299 (1988).

5. T. Kobayashi et al., Phys. Lett. **B232**, 51 (1989).
6. C.A. Bertulani and G. Baur, Nucl. Phys. **A480**, 615 (1988); C.A. Bertulani, G. Baur and M.S. Hussein, Nucl. Phys. **A526**, 751 (1991).
7. C.A. Bertulani and H. Sagawa, Nucl. Phys. A, **A588**, 667 (1995).
8. C.A. Bertulani, Phys. Rev. **C49**, 2688 (1994); Nucl. Phys. **A587**, 318 (1995).
9. T. Nakamura, Phys. Lett. **B331**, 296 (1994).
10. R. Anne et al., Zeit. Phys. **A352**, 397 (1995).
11. G.F. Bertsch and C.A. Bertulani, Nucl. Phys. **A556**, 136 (1993); Phys. Rev. **C49**, 2839 (1994); H. Esbensen, G.F. Bertsch and C.A. Bertulani, Nucl. Phys. **A581**, 107 (1995).
12. C.A. Bertulani, L.F. Canto and M.S. Hussein, Phys. Lett. **B353**, 413 (1995).
13. K. Alder and A. Winther, *Coulomb Excitation*, Academic Press, New York, 1965.
14. G.R. Satchler, Nuc. Phys. **A472**, 215 (1987).
15. C.A. Bertulani, L.F. Canto, M.S. Hussein, and A. de Toledo Piza, Phys. Rev. **C53**, 334 (1996).
16. K. Ieki et al., Phys. Rev. Lett. **70**, 730 (1993); D. Sackett et al., Phys. Rev. **C48**, 118 (1993).
17. C.A. Bertulani and L.F. Canto, Nucl. Phys. **A539**, 163 (1992); G. Baur, C.A. Bertulani and D. Kalassa, Nucl. Phys. **A550**, 527 (1992).
18. L.F. Canto, R. Donangelo, A. Romanelli and H. Schulz, Phys. Lett. **B318**, 415 (1993).

19. G. Baur, C.A. Bertulani and H. Rebel **A458**, 188 (1986).
20. T. Motobayashi et al. Phys. Rev. Lett. **73**, 2680 (1994).
21. M. Gai and C.A. Bertulani, Phys. Rev. **C52**, 1706 (1995); K. Suemmerer, accepted proposal for Coulomb breakup of 8B at the SIS, GSI/Darmstadt.
22. C.A. Bertulani and K.W. McVoy, Phys. Rev. **C46**, (1992) 2638; Phys Rev. **C48**, 2534 (1993); M.S. Hussein and K.W. McVoy, Nucl. Phys. **A445**, 124 (1985).
23. P. Banerjee and R. Shyam, Phys. Lett. **B349**, 421 (1995).
24. A.A. Korshennikov, M.V. Zhukov, M. H. Smedberg and T. Kobayashi, Europhys. Lett. **29**, 359 (1995).